ORGANOMETALLICS

Article

pubs.acs.org/Organometallics

Mechanism of Alkyl Migration in Diorganomagnesium 2,6-Bis(imino)pyridine Complexes: Formation of Grignard-Type Complexes with Square-Planar Mg(II) Centers

John J. Sandoval, Pilar Palma, Eleuterio Álvarez, Juan Cámpora,* and Antonio Rodríguez-Delgado*

Instituto de Investigaciones Químicas, CSIC − Universidad de Sevilla, C/Américo Vespucio, 49, 41092, Sevilla, Spain

Supporting Information

ABSTRACT: Dialkylmagnesium compounds $[MgR_2L_2]$ (R = *n*-Bu, L = none or R = Bn, L = THF) react with 2,6-bis(imino)pyridines (BIP) to afford different types of Mg(II) alkyl complexes, depending on the nature of R. For R = *n*-Bu, thermally stable products resulting from selective alkyl transfer to the pyridine nitrogen (N1) atom are obtained. However, NMR studies showed that the reaction of $[Mg(Bn)_2THF_2]$ with ^{iPr}BIP at −65 °C leads to a thermally unstable product arising from benzyl migration to position C2 in the pyridine ring. Above +5 °C, this compound rearranges, cleanly yielding a mixture of two isomeric complexes, in which the benzyl group has migrated to positions C3 or C4 of the central ring, respectively. Similar isomeric mixtures were obtained when $[Mg(Bn)_2THF_2]$ was reacted with ^{iPr}BIP or ^{Mes}BIP at room temperature. Such mixtures are thermally stable below 80 °C, but at this temperature, the 3-benzyl isomer converts into the thermodynamically favored 4-benzyl product, albeit not quantitatively. An alternate route was devised for the selective syntheses of the latter type of compounds. The X-ray diffraction structure of one of them provided an unusual example of a square-planar alkylmagnesium(II) center.

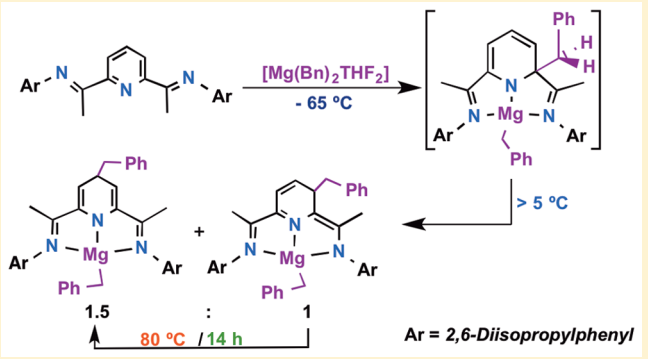

INTRODUCTION

Alkyl complexes supported by 2,6-bis(imino)pyridine (BIP) ligands attracted much interest over the last quarter-century,[1,2] mainly due to their role in olefin polymerization or oligomerization,[2e,3] and other catalytic processes.[4] The high-light has not been limited to transition metal derivatives, as the chemistry of main group alkyls with BIP ligands has also been investigated.[5,6] BIP-ligated alkyl complexes are also noteworthy compounds due to the unusual reactivity patterns imparted to the alkyl-metal fragment by noninnocent BIP ligands. The interaction of strongly π electron-acceptor BIP ligands with electron-rich MR_n fragments leads to the weakening of M−C bonds.[7] This effect explains why very few *poly*alkyls $[MR_n(BIP)]$ have been isolated, mainly dialkyls $[M(CH_2SiMe_3)_2(BIP)]$ (M = Fe[8] or Mn[2f]), whose M−C bonds are stabilized by β-silylated alkyl groups. Similar derivatives containing non-stabilized, β-H free R groups are much less stable and evolve spontaneously experiencing M−C fission. Although these processes can be complicated by unselective reactions at the BIP ligand,[1] under well-controlled conditions, alkyls of type $[MR_n(BIP)]$ evolve through the basic routes shown in Scheme 1, namely, M−R bond homolysis, affording reduced species of type $[MR_{n-1}(BIP)]$, or alkyl transfer to the pyridine ring, which leads to a range of products containing modified BIP ligands ($[MR_{n-1}(BIP')]$). M−R bond homolysis has been demonstrated for transition metals such as, e.g., iron,[2c,9] cobalt,[10] or manganese,[11] while alkyl migration is considerably more general, having been observed both for transition and main metal elements.

Scheme 1. Common Decomposition Routes Experienced by $[MR_n(BIP)]$ Complexes

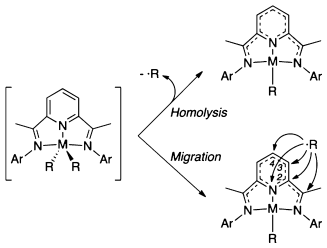

Although in general, unstable, polyalkyls $[MR_n(BIP)]$ can be readily generated in solution by reacting BIP ligands with suitable metal precursors, MR_n or $[MR_n(L')_m]$, where L′ represents labile, easily displaced coligands such as THF or Py. The evolution of such polyalkyl species and, more specifically, ·R migration to remote positions on the BIP ligand poses an interesting problem of selectivity control that could be influenced by steric effects, and the nature of both the migrating ·R group and the metal center. Such control ranges from poor (e.g., for MR_n = aluminum alkyls[6b]) to excellent. For example,

Received: July 11, 2016

DOI: 10.1021/acs.organomet.6b00528
Organometallics XXXX, XXX, XXX−XXX

Gibson studied the reactions of LiR, MgR_2, or ZnR_2 (R = Me, Et, Pr, *i*Pr) with a variety of BIP ligands, finding that, in favorable cases, they proceed with high selectivity.[5b] In such instances, the primary products invariably result from alkyl transfer from the metal to the pyridine N atom of the BIP ligand. In contrast, we have shown that dialkylmanganese BIP complexes (R = benzyl, allyl, neophyl, and trimethylsilylmethyl) undergo highly regioselective alkyl migration to the position 4 in the pyridine ring.[2f,12] Similar selectivity has also been noted for ·R migration to the pyridine ring in iron alkyl derivatives.[9b] Recent studies suggest that such divergent chemistries could be more influenced by the nature of the migrating R group than by the different character of the metal center. Thus, we have recently reported that the behavior of zinc alkyls $[ZnR_2(BIP)]$ with R = benzyl or allyl is similar to that of their Mn(II) analogues; i.e., they selectively transfer one R group not to the N atom of the pyridine ring, but to position 4, affording stable 1,4-dihydropyridinate complexes. A comparison between analogous Mn(II) and Zn(II) chemistries is meaningful, because these ions have inert $3d^5$ and $3d^{10}$ shells and similar covalent radii in their molecular compounds ($r_{cov,Mn}$ = 1.19 Å; $r_{cov,Zn}$ = 1.18 Å).[13] Mg(II) is the closest d^0 analogue of Mn(II) and Zn(II), although its size is somewhat larger ($r_{cov,Mg}$ = 1.39 Å). Thus, comparisons between Mn(II), Zn(II), and Mg(II) are also pertinent, especially considering the growing attention of alkaline-earth reagents in catalysis.[14] When studying the reaction of bulky alkaline-earth alkyls $[MR_2(THF)_n]$ (M = Ca, Sr, Ba; R = $CH(SiMe_3)_2$) with ^{iPr}BIP, Hill observed competitive R migration to positions 3 and 4 of the heterocyclic ring.[5b] These products are thermally unstable in solution at room temperature, and this leads to the elimination of 2 equiv of $CH_2(SiMe_3)_2$ by intramolecular H abstraction from the weakly acidic acetimidoyl (CH_3-CN) *arms* of the BIP ligand. Interestingly, for M = Mg, the reaction initially leads to a C_2-symmetrical adduct tentatively identified as the corresponding dialkyl $[MgR_2(^{iPr}BIP)]$, which only undergoes intramolecular deprotonation at 60 °C without forming ring-alkylated intermediates. In order to further clarify the reactivity of alkali-earth alkyls with BIP ligands, we decided to revisit the reaction of BIP ligands with MgR_2, specifically with previously unexplored R = *n*-Bu (but similar to those studied by Gibson) and Bn (benzyl), which is the Mg(II) analogue of the Mn and Zn benzyls that we investigated before.[2f,5a,12] For this purpose, we chose as starting material the THF solvate of dibenzylmagnesium, $[Mg(Bn_2)(THF)_2]$, reported by Schrock in 1976,[15] whose crystal structure has now been determined and is shown in the Supporting Information (Figure S3).

RESULTS AND DISCUSSION

Both the dibutyl and dibenzyl magnesium derivatives react instantly when treated with stoichiometric amounts of the bulky ligands ^{iPr}BIP or ^{Mes}BIP, affording structurally different products, depending on the nature of R (Scheme 2). In the case of $Mg(n\text{-}Bu)_2$, the ^{1}H NMR spectra of the deep purple reaction mixtures showed the formation of a single type of product, **1a** or **1b**. These are characterized by the high field shift of the H4 and 3,3′ signals of the pyridine ring, from the 7.50−9.00 ppm region where they appear in the spectra of the free ligands, to 6.80−5.50 ppm (see Figure S1, SI). This is reminiscent of the data reported by Gibson for the *N*-alkylated products $[Mg(R)(N\text{-}R\text{-}BIP)]$ generated from other dialkylmagnesium reagents (with R = Me, Et, *i*Pr) and various BIP ligands.[5c] The identity of the new compounds was confirmed with the

Scheme 2. Magnesium Dialkyls React with ^{iPr}BIP or ^{Mes}BIP Affording Structurally Different Products

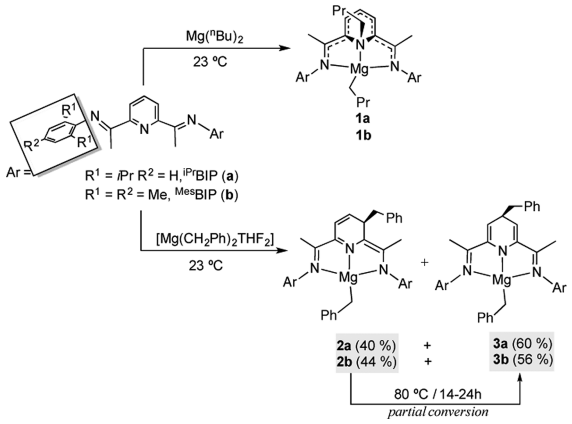

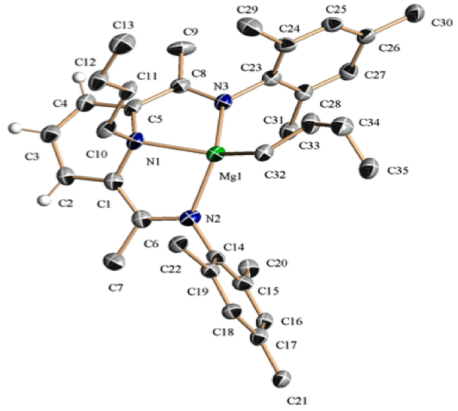

Figure 1. ORTEP representation of the structure of **1b**. Selected bond lengths (Å) and angles (deg): Mg(1)−C(32), 2.171(14); Mg(1)−N(1), 2.171(11); Mg(1)−N(2), 2.112(13); Mg(1)−N(3), 2.116(13); N(1)−C(10), 1.518 (14); N(1)−C5, 1.445 (18); N(1)−C1, 1.451 (14); C1−C2, 1.40 (2); C2−C3, 1.44 (2); C1−C6, 1.39 (2); C6−C7, 1.51(2); N(1)−Mg(1)−C(32), 139.5; N(1)−Mg(1)−N(2), 80.7(5); N(1)−Mg(1)−N(3), 76.8(5); N(2)−Mg(1)−N(3), 129.6(4); N(2)−Mg(1)−C(32), 109.0(6); N(3)−Mg(1)−C(32), 117.6(6).

structural characterization of **1b**, shown in Figure 1. Its general features and crystal bond lengths and angles show no significant differences with those of Gibson's compounds.[5c] The geometry of the Mg atom in this kind of complexes could be described as a flattened tetrahedron, i.e., intermediate between tetrahedral and square planar. The geometric parameter τ_4[16] for the Mg center in **1b** is 0.65. This parameter takes the value 1 for the tetrahedron and 0 for square-planar geometry; therefore, the metal center is closer to tetrahedral. Complexes **1** are stable in solution up to 40 °C but undergo unselective isomerization on heating at 60 °C (**1b**: ca. 40% *n*-Bu migration from N to position 2 after 24 h).

Treatment of $[Mg(Bn)_2(THF)_2]$ solutions with stoichiometric amounts of ^{iPr}BIP or ^{Mes}BIP in C_6D_6 induces an instantaneous color change to dark blue. The ^{1}H NMR spectra of these solutions appear more complex than those of compounds **1** (see Figure S2 in the SI) due to the formation of two products, **2a**/**b** or **3a**/**b**, respectively. Otherwise, both reactions are very clean and no side products are detected in the spectra. The identity of the products was unambiguously established on the basis of their NMR spectra, ^{1}H and ^{13}C, bidimensional ^{1}H−^{1}H COSY, and ^{1}H−^{13}C heterocorrelations.

DOI: 10.1021/acs.organomet.6b00528
Organometallics XXXX, XXX, XXX−XXX

As shown in Scheme 2, **2** and **3** are isomeric complexes arising from competitive migration of one benzyl group to positions 3 and 4 in the pyridine ring, respectively. The ^{1}H NMR spectra of isomers **3** display diagnostic multiplets at δ 4.13 (**3a**) or 4.16 ppm (**3b**) corresponding to the aliphatic methyne 4-C(Bn)*H* of their 1,4-dihydropyridinate fragments, which split as multiplets (ideally, triplet of triplets) by coupling to the equivalent sp^2 methynes 3 and 3′-C*H* (doublets at δ 5.02 for **3a** or 5.04 for **3b**), and to the benzyl methylene group (doublets at δ 2.86 and 2.91 for **3a** and **3b**, respectively). The spectra of isomers **2a**/**b** are more complex than those of **3a**/**b**, due to the breakdown of molecular symmetry caused by the Bn in position 3. The 4-C*H* methynes of the central ring split as doublets of doublets placed at δ 5.25 (**2a**) or 5.29 (**2b**) due to differential coupling with the aliphatic 3-C(Bn)*H* and the sp^2 5-C*H* ($^3J_{HH} \approx 6$ and 9 Hz). In addition, the asymmetry of the 3-C(Bn)*H* centers causes the benzyl CH_2 protons to become diastereotopic. According to ^{1}H NMR integrals, isomers **3** are slightly more abundant than **2**, even when benzyl migration to position 3 is twice as likely than migration to 4. Considering this statistical factor, the selectivity ratios for migration to 3 vs 4 are 1:3 for ^{iPr}BIP and 1:1.5 for ^{Mes}BIP. The similar values indicate that the steric bulk of the aryl substituents have little influence on the migration selectivity.

The outcome of the reactions of dibenzylmagnesium with BIP ligands stands in stark contrast with the selective formation of *N*-alkylated species from Mg(*n*-Bu)$_2$ or other dialkylmagnesiums reported by Gibson, but is akin to Hill's results with the bulky bis(trimethylsilylmethyl) derivatives of Ca, Sr, and Ba.[5b] As mentioned above, the heavier alkali-earth analogues of **2** and **3** eliminate 2 equiv of alkane upon standing in solution at room temperature. We heated the C_6D_6 solutions containing the **2a**/**3a** isomeric mixture, but no significant changes were observed in the ^{1}H spectra after 48 h at 60 °C. However, the **2a**:**3a** isomeric ratio gradually shifts at 80 °C, becoming 1:9 after heating for 14 h. A similar, but slower, isomerization process was observed in the ^{Mes}BIP system, which attains a **2b**:**3b** ratio of 1:2 under the same conditions. No further shift was observed when the heating was continued for 24 h, but signs of decomposition started to show up in both cases.

Since the reactions of BIP ligands with dibenzylmagnesium do not afford single products, we envisioned a straightforward method to prepare derivatives of type **3**. This method involves the reaction of magnesium dialkyls with the benzylated 1,4-dihydropyridine 4-Bn-^{iPr}H$_2$BIP, as shown in Scheme 3. To this purpose, we optimized our Mn-based methodology[12] to prepare the dihydropyridine ligand free from the aromatized 4-Bn-^{iPr}BIP (see the Experimental Section). As anticipated, [Mg(Bn$_2$)(THF)$_2$] reacts cleanly and selectively with 4-Bn-^{iPr}H$_2$BIP, yielding a dark purple microcrystalline solid whose NMR spectra were undistinguishable from those of the **3a** component in the **2a**/**3a** mixture. Complex **3a** turns out to be thermally stable and does not isomerize appreciably to **2a** when heated in solution at 80 °C for 48 h. This means that the isomeric ratio 1:9 attained after heating the **2a**/**3a** mixture (and most likely **2b**/**3b** as well) is not determined by a chemical equilibrium, but is a limiting value due to the slowness of the isomerization process.

In spite of preparing **3a** selectively, we were unable to grow X-ray quality crystals of this compound. However, reacting Mg(*n*-Bu)$_2$ with 4-Bn-^{iPr}H$_2$BIP leads to the corresponding *n*-butylmagnesium-dihydropyridinate **4**, whose crystal structure is shown in Figure 2. Although similar complexes are known to arise from selective migration of alkyl to BIP ligands,[2f,5b,6b,9b] so far the only structurally characterized example is the Zn(II) analogue of **3a** that we reported a few years ago.[5a] In the latter compound, the dihydropyridinate ligand favors a square-planar geometry at the Zn(II) center (τ_4 = 0.32), and a similar configuration is observed in **4** (as in other structurally analogous square-planar Al(III) complexes recently reported[17]), although, in this case, the carbon atom bound to Mg departs slightly from planarity. This deviation is small, but gives rise to a crystallographic disorder, as the Mg−C vector can take two possible orientations, forming angles of 26° (configuration A) or −32° with the main coordination plane (configuration B). Both possible values of τ_4, 0.40 (A) or 0.44 (B), indicate that the geometry of the Mg(II) center is closer to square-planar than in the structure of **1b**. Several square-planar Mg(II) coordination complexes containing macrocyclic[18] or polydentate ligands[6,19] have been reported, but this is unprecedented for Grignard-type compounds. Interestingly, the Mg−C bond is significantly longer in **4** (2.240(12) Å) than in **1b** (2.151(14) Å), although the Mg-bound *n*-Bu poses no important steric hindrance. The difference could be attributed to the different character of the N donors placed in *trans*, which is amide, covalent-type in **4** and amino, dative-type, in **1b**. If this interpretation were correct,[20] this would be a highly unusual case of *trans influence* in a square-planar magnesium complex.

Scheme 3. Direct and Selective Synthesis of Dihydropyridinate Magnesium Alkyls

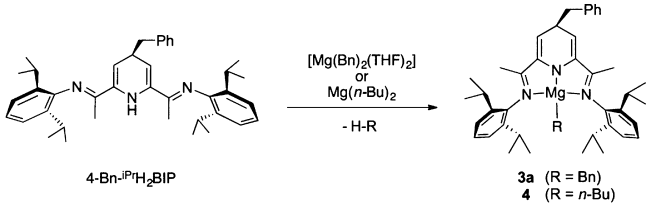

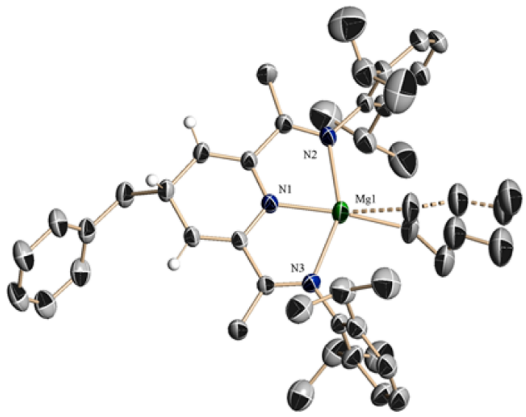

Figure 2. ORTEP representation of the structure of compound **4**, showing the disorder of the *n*-Bu ligand. Selected bond lengths (Å) and angles (deg): Mg(1)−C(41A), 2.240(12); Mg(1)−N(1), 1.989(4); Mg(1)−N(2), 2.231(5); Mg(1)−N(3), 2.241(5); N(1)−C(5), 1.369 (6); N(1)−C1, 1.363(6); C1−C2, 1.348 (7); C2−C3, 1.498(8); C1−C6, 1.464 (7); C6−C7, 1.508(8); N(1)−Mg(1)−C(41A), 154.0(5); N(1)−Mg(1)−C(41B), 157.8(9); N(1)−Mg(1)−N(2), 74.83(17); N(1)−Mg(1)−N(3), 74.85(17); N(2)−Mg(1)−C(41A), 101.2(4); N(2)−Mg(1)−N(3), 149.69 (18); N(3)−Mg(1)−C(41A), 106.1(4); N(1)−Mg(1)−C(41A), 154.0(5).

DOI: 10.1021/acs.organomet.6b00528
Organometallics XXXX, XXX, XXX−XXX

In order to gain further insight on the mechanism of the reaction of MgR_2 with BIP ligands, we monitored the interaction of $[Mg(Bn)_2(THF)_2]$ with ^{iPr}BIP using variable temperature ^{1}H NMR between −60 and +25 °C (Figure 3).

Scheme 4. Reaction of ^{iPr}BIP with Isolated $[Mg(Bn)_2(THF)_2]$

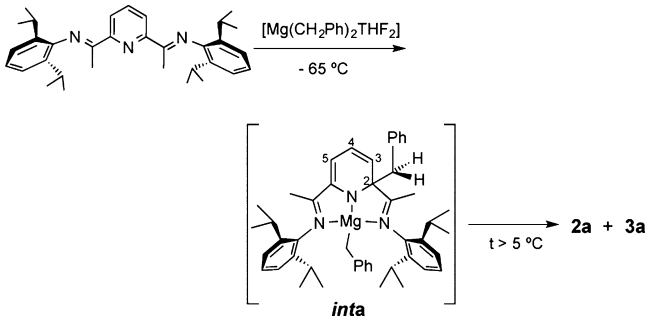

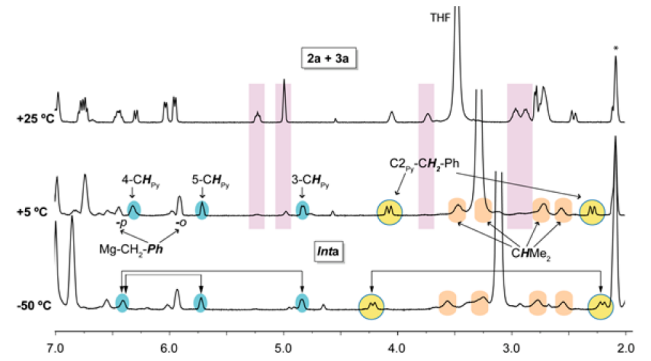

Figure 3. ^{1}H NMR monitoring of the reaction of equimolar amounts of ^{iPr}BIP with $[Mg(Bn)_2(THF)_2]$ in toluene-d_8. For clarity, only the central regions of the spectra are shown. Arrows in the bottom spectrum indicate the most relevant ^{1}H−^{1}H couplings detected in the COSY spectrum at −50 °C. See-through bands highlight "growing" signals of the final products **2a** and **3a**. The asterisk marks the residual signal of the deuterated solvent.

When the ligand is added to a toluene-d_8 solution of the Mg reagent cooled at −65 °C, a rapid color change ensues, from yellow to green. The ^{1}H NMR spectrum recorded at −60 °C indicates full conversion of the starting materials. Careful analysis of the spectrum at −50 °C (whose resolution was better than at −60 °C) indicates the presence of several species, although one of them, intermediate ***inta***, is clearly prevalent. Little change is observed as the sample is warmed from −60 to 0 °C, but at +5 °C, the signals of **2a**/**3a** begin to be noticeable (transparent highlighted bars in Figure 3). Further warming at room temperature caused the original spectrum to be fully replaced by that of **2a**/**3a**, indicating that all species present in the original mixture share the same fate.

The spectrum of ***inta*** is not as simple as it would be anticipated for a symmetric dialkyl $[MgBn_2(^{iPr}BIP)]$, analogous to those observed in the reactions of ^{iPr}BIP with $Zn(Bn)_2$ at low temperature,[5a] or with $Mg(CH(SiMe_3)_2)_2$ at 23 °C.[5b] A distinct feature of this spectrum is a pair of doublets at δ 2.24 and 4.27 ppm due to an AX spin system with J_{AX} = 14 Hz (confirmed in the COSY spectrum). The large J_{AX} constant is consistent with geminal rather than vicinal coupling; therefore, it was assigned to a diastereotopic pair of methylene protons belonging to one of the benzyl groups. This points to a low symmetry species, as supported by the observation of four signals between 2.50 and 4.00 ppm corresponding to methyne groups of the four inequivalent *i*Pr groups of the ^{iPr}BIP ligand. The COSY spectrum provides further valuable indications of coupling relationships (sketched in the bottom spectrum of Figure 3) between three poorly resolved multiplets placed at 4.84, 5.72, and 6.42 ppm, each of them integrating for 1H. These signals were assigned to the H3, H4, and H5 protons of the dearomatized pyridine ring arising from benzyl migration to position 2, as indicated in Scheme 4. The data for similar Mg, Zn, and Al complexes reported in the literature match well those of ***inta*** (4.7−5.1, 5.4−5.6, and 6.0−6.3 ppm, respectively).[5c,6b] In addition, Gambarotta reported a similar paramagnetic Fe(II) complex arising as a minor byproduct from the alkylation of $[FeCl_2BIP]$ with $LiCH_2SiMe_3$.[21] All of these compounds are stable at room temperature. In contrast, the observed lability of ***inta*** at +5 °C indicates a very low energy barrier for its isomerization to **2a** or **3a**, estimated in 18−19 kcal/mol. As a comparison, the estimated energy barrier for the isomerization of **2a** to **3a**, which takes place over several hours at 80 °C, is 27−28 kcal/mol.

The facile transformation of ***inta*** in **2a** and **3a**, and the irreversible isomerization of **2a** into **3a**, indicates that the thermodynamic preference of the pyridine alkylation increases in the order 2 < 3 < 4. On the other hand, the significant difference between the energy barriers for isomerizations ***inta*** → **2a** and **2a** → **3a** means that **2a** cannot be an intermediate in the route ***inta*** → **3a**, that is, the benzyl group must "jump" directly from position 2 to 4. A concerted 2,4-shift cannot be excluded, but, very likely, R shifts within the BIP ligand involve transitory formation of free ·R radicals.[7a] This helps explain why benzyl is more prone than normal alkyls such as *n*-Bu to migrate to remote positions in the pyridine ring, since the stabilized benzyl free radical is more easily formed.

CONCLUSIONS

In summary, we have studied the reactions of magnesium dialkyls (MgR_2) (R = *n*-Bu, Bn) with ^{iPr}BIP or ^{Mes}BIP ligands and demonstrated that the result is critically influenced by the nature of the R group. The size of the aryl substituents of the BIP ligand has little impact in the process. For R = *n*-Bu, one alkyl group is selectively transferred to the central nitrogen in the pyridine ring, giving rise to remarkably stable monoalkyl complexes. In contrast, when R = Bn, competitive migration to positions 3 and 4 is observed at room temperature, affording mixtures of complexes of types **2** and **3**. These species are formed under kinetic control, but on heating, 3-benzyl-enaminates **2** isomerize into the thermodynamically more stable 4-benzyl-1,4-dihydropyridinate complexes **3**. Variable temperature NMR shows that, at −60 °C, the benzyl group migrates preferentially to position 2, giving rise to the 2-benzyl-1,2-dihydropyridinate ***inta***. Above 0 °C, this compound readily rearranges to the mixture of products observed at room temperature. On the basis of these observations, we established a qualitative order of thermodynamic stabilities, being the compound alkylated in position 4 of the central pyridine the most stable, and the one on position 2 the least. Since the reactions of BIP ligands with $[Mg(Bn)_2(THF)_2]$ do not afford single products, we developed a convenient route for the selective synthesis of alkylmagnesium dihydropyridinate complexes **3a** and **4**. The crystal structure of the latter provides an unusual example of square-planar coordination in a Grignard-type magnesium complex.

DOI: 10.1021/acs.organomet.6b00528
Organometallics XXXX, XXX, XXX−XXX

EXPERIMENTAL SECTION

General Considerations. All manipulations were carried out under an oxygen-free argon atmosphere, using conventional Schlenk techniques or a nitrogen-filled glovebox. Solvents were rigorously dried and degassed prior use. Methanol was refluxed over sodium methoxide, distilled, and kept in a Teflon screw-cap glass ampule over activated molecular sieves. NMR spectra were recorded on Bruker Avance III-400 and DRX-500 spectrometers (FT 400 and 500 MHz, ^{1}H; 100 and 125 MHz, ^{13}C). The ^{1}H and ^{13}C{^{1}H} resonances of the solvent were used as the internal standard, but the chemical shifts are reported with respect to TMS. Spectral assignations were routinely helped with monodimensional ^{13}C (gated), DEPT 135 and 2D ^{1}H−^{1}H COSY, and ^{1}H−^{13}C HSQC and HMBC heterocorrelation spectra. NMR-scale reactions (typically in a 0.02 mmol scale) were conducted in NMR tubes sealed with Teflon J. Young-type screw-cap valves. Benzene-d_6 and toluene-d_8 were dried over sodium benzophenone ketyl and vacuum-distilled. The Microanalytical Service of the Instituto de Investigaciones Químicas carried out the elemental microanalyses.

Mg(^{n}Bu)$_2$ and Mg(Bn)Cl were purchased from Sigma-Aldrich, being both titrated prior to use. Derivatives 2,6-[2,6-^{i}Pr$_2$C$_6$H$_3$N═C(Me)]$_2$C$_5$H$_3$N (^{iPr}BIP) and 2,6-[2,4,6-Me$_3$C$_6$H$_2$N═C(Me)]$_2$C$_5$H$_3$N (^{Mes}BIP) were prepared according to conventional procedures that involve the condensation of 2,6-diacetylpyridine with the corresponding anilines under azeotropic water-removal conditions.

Preparation of [Mg(Bn)$_2$THF$_2$]. This compound was prepared adapting a method reported by Schrock,[15] which is described as follows. To a stock solution of Mg(Bn)Cl (0.90 M, 48 mL, 36.0 mmol) in Et$_2$O, stirred at −40 °C, 10 mL of a dioxane solution in the same solvent (3.6 M, 36.0 mmol) was added dropwise. The mixture was allowed to warm to room temperature, and the stirring was continued for 5 h. The resultant white suspension was centrifuged. The supernatant liquid was transferred via cannula to an oxygen- and moisture-free oven-dried flask, and the colorless solution was evaporated and dried under vacuum overnight. The resultant white solid was then redissolved in 10 mL of THF, and pentane (5 mL approx.) was added until the solution became slightly turbid. Colorless crystals suitable for X-ray diffraction studies corresponding to [**Mg(Bn)$_2$THF$_2$**] appeared after storing the solution for several days at −25 °C. Upon filtration and drying, 4.42 g (35%) of a crystalline white solid was obtained. Its crystal structure is shown in the Supporting Information (Figure S3) together with selected bond distances and angles. ^{1}H NMR (C$_6$D$_6$, 25 °C, 400 MHz), δ 1.06 (m, 8H, CH_2 (2,5)-THF), 1.84 (s, 4H, Mg-Bn), 3.17 (m, 8H, CH_2 (3,4)-THF), 6.76 (t, 2H, $^3J_{HH}$ = 7.1 Hz, p-CH_{ar} Bn), 7.10 (d, 4H, $^3J_{HH}$ = 7.5 Hz, o-CH_{ar} Bn), 7.18 (overlapping signal of residual benzene and 4H, m-CH_{ar} Bn). ^{13}C{^{1}H} NMR (C$_6$D$_6$, 25 °C), δ 22.9 (Mg-Bn), 24.7 (CH$_2$ (3,4)-THF), 68.9 (CH$_2$ (2,5)-THF), 116.1 (p-CH$_{ar}$ CH$_2$$Ph$), 123.4 ($o$-CH$_{ar}$ Bn), 128.1 (m-CH$_{ar}$ Bn), 156.9 (i-C$_{ar}$ Bn). Anal. Calcd for C$_{22}$H$_{30}$MgO$_2$: C, 75.33; H, 8.62. Found: C, 75.00; H, 8.58.

Synthesis of [Mg(n-Bu)(N-n-Bu-^{iPr}BIP)] (1a). To a cold (−70 °C) suspension of ^{iPr}BIP (927.0 mg, 1.92 mmol) in toluene (40 mL), a solution of Mg(^{n}Bu)$_2$ (1.06 M, 2.0 mL, 2.12 mmol) in heptane was added via syringe. The color of the mixture changed from yellow to blue-purple. After 10 min, the cooling bath was removed and the mixture was stirred overnight at room temperature. All volatiles were removed under vacuum, leaving a blue-purple oil, whose ^{1}H NMR showed a single set of signals that corresponds to compound **1a** (Figure S1, SI). The solid was dissolved in pentane (15 mL), concentrated until 1/3 of its initial volume, and stored at −25 °C. After 3 days, compound **1a** precipitated as purple solid. Upon filtration and drying, 772.0 mg (65%) of **1a** was isolated. ^{1}H NMR (C$_6$D$_6$, 25 °C, 400 MHz), δ −0.27 (bs, 2H, α-CH_2 Mg^nBu), 0.78 (bs, 3H, CH_3 Mg^nBu), 0.88 (t, 3H, $^3J_{HH}$ = 7.3 Hz, CH_3 N^nBu), 1.02 (d, 6H, $^3J_{HH}$ = 6.7 Hz, CHMe_2), 1.12 (d, 6H, $^3J_{HH}$ = 6.8 Hz, CHMe_2), 1.14−1.25 (overlapping signals, 4H, γ-CH_2 N-^{n}Bu, γ-CH_2 Mg-^{n}Bu assigned by COSY 2D-^{1}H−^{1}H), 1.24 (d, 6H, $^3J_{HH}$ = 6.8 Hz, CHMeMe), 1.28−1.39 (m, 2H, β-CH_2 Mg-^{n}Bu, overlapping with signals of CHMe_2), 1.40 (d, 6H, $^3J_{HH}$ = 6.6 Hz, CHMe_2), 1.68 (s, 6H, Me-CN), 1.90 (m, 2H, β-CH_2 N-^{n}Bu), 2.84−2.89 (overlapping signals, 4H, α-CH_2 N-^{n}Bu and CHMe$_2$), 3.17 (sept, 2H, $^3J_{HH}$ = 6.9 Hz, CHMe$_2$), 5.48 (t, 1H, $^3J_{HH}$ = 7.3 Hz, 4-CH_{Py}), 6.78 (d, 2H, $^3J_{HH}$ = 7.3 Hz, 3,3′-CH_{Py}), 7.08−7.17 (m, 6H CH_{Ar} N-Aryl, overlapping with residual signal of C$_6$D$_6$). ^{13}C{^{1}H} NMR (C$_6$D$_6$, 25 °C, 100 MHz), δ 8.8 (α-CH$_2$ Mg^{n}Bu), 14.8 (δ-CH$_3$ Mg^{n}Bu), 14.8 (δ-CH$_3$ Mg-^{n}Bu), 14.9 (δ-CH$_3$ N-^{n}Bu), 17.0 (Me-C═N), 21.7 (γ-CH$_2$ N-^{n}Bu), 24.4, 24.7, 24.8, 25.0 (CH$Me$$Me$), 29.1 (CHMe$_2$), 29.2 ($\gamma$-CH$_2$ N-^{n}Bu), 29.7 (CHMe$_2$), 29.8 (β-CH$_2$ N-^{n}Bu) 32.6 (β-CH$_2$ Mg^{n}Bu), 53.0 (α-CH$_2$ N-^{n}Bu), 104.4 (4-CH$_{Py}$), 118.1 (2,2′-C$_{Py}$), 124.0, 124.5 (m-CH$_{N\text{-}Ar}$), 126.1 (p-CH$_{N\text{-}Ar}$), 132.0 (3-CH$_{Py}$), 140.9, 142.7 (o-C$_{N\text{-}Ar}$), 145.3 (i-C$_{N\text{-}Ar}$), 170.7 (Me-CN). Anal. Calcd for C$_{41}$H$_{61}$MgN$_3$: C, 79.39; H, 9.91; N, 6.77. Found: C, 78.89; H, 10.43; N, 7.24.

Synthesis of [Mg(n-Bu)(N-n-Bu-^{Mes}BIP] (1b). The same experimental procedure described above for the synthesis of compound **1a** was applied to prepare compound **1b**, starting from 1030 mg (2.6 mmol) of ^{Mes}BIP. Crystallization of the crude product from hexane (10 mL) at −20 °C yielded 794 mg (57%) of a purple microcrystalline material. Single crystals suitable for X-ray diffraction studies were obtained from a concentrated hexane solution of **1b** at −25 °C. ^{1}H NMR (C$_6$D$_6$, 25 °C, 400 MHz), δ −0.06 (t, 2H, $^3J_{HH}$ = 7.6 Hz, α-CH_2 Mg^nBu), 0.76 (t, 3H, $^3J_{HH}$ = 7.2 Hz, CH_3 Mg^nBu), 0.88 (t, 2H, $^3J_{HH}$ = 7.3 Hz, CH_3 N-^{n}Bu), 1.06 (quint, 2H, $^3J_{HH}$ = 7.2 Hz, γ-CH_2 Mg^nBu), 1.19 (quint, 2H, $^3J_{HH}$ = 7.5 Hz, γ-CH_2 N-^{n}Bu), 1.54 (quint, 2H, $^3J_{HH}$ = 7.5 Hz, β-CH_2 Mg^nBu), 1.60 (s, 6H, Me-CN), 1.90 (overlapping signals, 8H, 2 × o-$Me$$_{N\text{-}Ar}$ and β-CH_2 N-^{n}Bu), 2.13 (s, 6H, o-$Me$$_{N\text{-}Ar}$), 2.23 (s, 6H, p-$Me$$_{N\text{-}Ar}$), 2.77 (m, 2H, α-CH_2 N-^{n}Bu), 5.59 (t, 1H, $^3J_{HH}$ = 7.3 Hz, 4-CH_{Py}), 6.76 (s, 2H, m-C$H_{N\text{-}Ar}$), 6.80 (d, 2H, $^3J_{HH}$ = 7.3 Hz, 3-CH_{Py}), 6.82 (s, 2H, m'-C$H_{N\text{-}Ar}$). ^{13}C{^{1}H} NMR (C$_6$D$_6$, 25 °C, 100 MHz), δ 9.4 (α-CH$_2$ Mg-^{n}Bu), 14.6 (CH$_3$ Mg-^{n}Bu), 14.9 (CH$_3$ N-^{n}Bu), 15.4 (Me-CN), 19.2, 19.6 (o-$Me$$_{N\text{-}Ar}$), 21.3 ($p$-$Me$$_{N\text{-}Ar}$), 21.5 ($\gamma$-CH$_2$ N-^{n}Bu), 29.3 (γ-CH$_2$ Mg-^{n}Bu), 32.3 (β-CH$_2$ N-^{n}Bu), 32.8 (β-CH$_2$ Mg-^{n}Bu), 51.5 (α-CH$_2$ N-^{n}Bu), 105.2 (4-CH$_{Py}$), 116.5 (2-C$_{Py}$), 129.5 (3-CH$_{Py}$), 129.7 (o-C$_{N\text{-}Ar}$), 130.1, 130.7 (m-CH$_{N\text{-}Ar}$), 132.1 (o'-C$_{N\text{-}Ar}$), 134.0 (p-C$_{N\text{-}Ar}$), 144.7 (i-C$_{N\text{-}Ar}$), 169.9 (Me-CN). Anal. Calcd for C$_{35}$H$_{49}$MgN$_3$: C, 78.42; H, 9.21; N, 7.84. Found: C, 78.36; H, 9.68; N, 7.51.

Reaction of [Mg(Bn)$_2$THF$_2$] with ^{iPr}BIP. Formation of [Mg(Bn)(4-Bn-^{iPr}HBIP)] (2a) and [Mg(Bn)(4-Bn-^{iPr}HBIP)] (3a). In a nitrogen filled glovebox, a colorless, cooled (5 °C) solution of [Mg(Bn)$_2$THF$_2$] (19.3 mg; 0.055 mmol) in 0.4 mL of C$_6$D$_6$ was added to a yellow suspension of ^{iPr}BIP (24.0 mg, 0.050 mmol) in the same solvent (0.4 mL) at 5 °C, placed in a 5 mL scintillation vial. The color of the reaction mixture changed instantaneously to dark green, and then, in less than 2 min, the solid had dissolved to give a dark blue solution. This was transferred to a screw-cap J. Young NMR tube and analyzed by ^{1}H NMR. The reaction was found to be complete, the spectrum showing two sets of signals corresponding to a mixture of complexes **2a** and **3a**, in a relative ratio of 1:1.5 (**2a**/**3a**) (see Figure S2, SI). The evolution of the mixture was monitored for a period of 7 h. No color changes and no evidence for changing were observed. In two separated experiments, similar samples were prepared and their evolution studied at 60 and 80 °C, respectively. Complex **2a**: ^{1}H NMR (C$_6$D$_6$, 25 °C, 400 MHz), δ 0.97 (d, $^3J_{HH}$ = 6.7 Hz, 3H, CHMeMe), 1.01 (d, $^3J_{HH}$ = 6.7 Hz, 3H, CHMeMe), 1.05 (d, $^3J_{HH}$ = 6.8 Hz, 3H, CHMeMe), 1.06 (d, $^3J_{HH}$ = 6.8 Hz, 3H, CHMeMe), 1.22−1.36 (12H, CHMeMe, overlapping signal with CHMeMe of complex **3a**), 1.28 (s, 3H, Me-CN), 1.69 (s, 3H, Me-CN), 1.83 (s, 2H, Mg-Bn), 2.47 (dd, 1H, $^3J_{HH}$ = 12.6, 3.5 Hz, CHH Py-Bn), 2.79 (m, 1H, CHH Py-Bn, hidden under the signal CHMe$_2$ of complex **3a**; identified by 2D ^{1}H−^{1}H COSY), 2.88 (m, 2H, CHMe$_2$), 2.98 (m, 2H, CHMe$_2$), 3.76 (m, 1H, 3-CH_{Py}), 5.25 (dd, 1H, $^3J_{HH}$ = 9.2, 5.8 Hz, 4-CH_{Py}), 6.14 (d, 2H, $^3J_{HH}$ = 7.6 Hz, o-CH_{Ar} Mg-Bn), 6.30 (d, 1H, $^3J_{HH}$ = 9.3 Hz, 5-CH_{Py}), 6.55 (t, 1H, $^3J_{HH}$ = 7.3 Hz, p-CH_{Ar} Mg-Bn), 6.88 (t, 2H, $^3J_{HH}$ = 7.7 Hz, m-CH_{Ar} Mg-Bn), 7.06−7.25 (m, 11H, C$H_{N\text{-}Ar}$ and CH_{Ar} Py-Bn). ^{13}C{^{1}H} NMR (C$_6$D$_6$, 25 °C, 100 MHz), δ 18.0 (Me-CN), 18.4 (Me-CN), 23.5 (CH$_2$, Mg-Bn), 23.8, 24.1, 24.2, 24.2 (CHMeMe), 24.9, 25.0, 25.0, 25.3 (CHMeMe), 28.4, 28.6 (CHMe$_2$ hidden under signals of **2a**), 38.5 (3-CH$_{Py}$), 44.9 (broad signal, CH$_2$ Py-Bn), 120.9 (5-CH$_{Py}$), 123.8, 124.0, 124.6, 125.3, 125.6, 126.6, 128.6, 128.7, 130.1 (CH$_{N\text{-}Ar}$, CH$_{Py}$, CH$_{Ar}$, Mg-Bn, Py-Bn), 138.6 (i-C$_{Ar}$, Py-Bn), 141.1,

DOI: 10.1021/acs.organomet.6b00528
Organometallics XXXX, XXX, XXX−XXX

146.6, 146.7 ($C_{N\text{-}Ar}$ or C_{Py}), 157.4 (*i*-C_{ar} Mg-Bn), 158.1 ($C_{N\text{-}Ar}$ or C_{Py}), 166.7 (PyC(Me)=NAr), 170.77 (broad, PyC(Me)=N-Ar). Complex **3a** (Signals lists and assignations confirmed with the spectra of isolated product; see later.): ^{1}H NMR (C_6D_6, 25 °C, 400 MHz), δ 0.98 (d, 6H, $^3J_{HH}$ = 6.7 Hz, CHMe_2), 1.02 (d, 6H, $^3J_{HH}$ = 6.7 Hz, CHMe_2), 1.28 (d, 12H, $^3J_{HH}$ = 6.9 Hz, CHMe_2), 1.64 (s, 2H, CH_2 Mg-Bn), 1.76 (s, 6H, *Me*C=N), 2.74 (broad septet, 4H, $^3J_{HH}$ = 4.1 Hz, CHMe$_2$), 2.86 (d, 2H, $^3J_{HH}$ = 6.8 Hz, CH_2 Py-Bn), 4.13 (m, 1H, 4-CH_{Py}), 5.02 (d, 2H, $^3J_{HH}$ = 3.9 Hz, 3,3′-CH_{Py}), 6.07 (d, 2H, $^3J_{HH}$ = 7.6 Hz, *o*-CH_{Ar} Mg-Bn), 6.53 (t, 1H, $^3J_{HH}$ = 6.8 Hz, *p*-CH_{Ar} Mg-Bn), 6.85 (t, 2H, $^3J_{HH}$ = 7.2 Hz, *m*-CH_{Ar} Mg-Bn), 6.99–7.19 (m, 11H, C$H_{N\text{-}Ar}$ and CH_{Ar} Py-Bn). ^{13}C{^{1}H} NMR (C_6D_6, 25 °C, 100 MHz), δ 17.4 (*Me*-C=N), 23.6 (CH_2 Mg-Bn), 23.7, 24.7, 24.8 (CHMe_2), 28.5, 28.6 (*C*HMe$_2$), 40.5 (4-CH_{Py}), 49.7 (CH_2 Py-Bn), 103.4 (3,3′-CH_{Py}), 115.7 (*p*-CH_{Ar} Mg-Bn), 124.0, 124.3 (*m*-$CH_{N\text{-}Ar}$), 124.5 (*o*-CH_{Ar} Mg-Bn), 125.9 (*m*-CH_{Ar} Py-Bn), 126.3 (*m*-CH_{Ar} Mg-Bn), 128.5 (*o*-CH_{Ar} Py-Bn), 128.6 (*p*-CH_{Ar} Py-Bn), 130.0 (*p*-CH_{Ar}), 138.7, 138.9 (*o*-$C_{N\text{-}Ar}$), 139.9 (*i*-C_{Ar} Py-Bn), 145.2 (2-C_{Py}), 145.6 (*i*-$C_{N\text{-}Aryl}$), 158.1 (*i*-C_{Ar} Mg-Bn), 173.4 (Me-*C*=N).

Reaction of [Mg(Bn)$_2$THF$_2$] with ^{Mes}BIP. Formation of [Mg(Bn)(4-Bn-^{Mes}HBIP)] (2b) and [Mg(Bn)(4-Bn-^{Mes}HBIP)] (3b). The same experimental protocol than the one described for the formation of **2a** and **3a** was set to investigate the reaction of [Mg(Bn)$_2$THF$_2$] with ^{Mes}BIP. The initial color of the reaction mixture was brown, and a little later it changed to deep blue. The ^{1}H NMR spectrum showed that the reaction was completed by the presence of just two set of new signals, which were attributed to compounds **2b** and **3b** with a relative of ratio of 1:1.2. The solution was monitored by ^{1}H NMR for 7 h, and no further changes were observed. Separated experiments were carried out to determine the evolution of the mixture at 60 and 80 °C. Complex **2b**: ^{1}H NMR (C_6D_6, 25 °C, 400 MHz), δ 1.48 (s, 3H, *Me*-CN), 1.54 (s, 2H, CH_2 Mg-Bn), 1.61 (s, 3H, *Me*-CN), 1.96 (s, 3H, *o*-$Me_{N\text{-}Ar}$), 2.00 (s, 3H, *o*-$Me_{N\text{-}Ar}$), 2.07 (s, 3H, *o*-$Me_{N\text{-}Ar}$), 2.08 (s, 3H, *o*-$Me_{N\text{-}Ar}$), 2.42 (s, 6H, *p*-$Me_{N\text{-}Ar}$), 2.48 (dd, 1H, $^3J_{HH}$ = 12.6, 4.8 Hz, CH*H* Py-Bn), 2.70 (dd, 1H, $^3J_{HH}$ = 12.5, 8.3 Hz, CH*H* Py-Bn), 3.76 (dd, 1H, $^3J_{HH} \approx {}^3J_{HH}$ = 6.0 Hz, 3-CH_{Py}), 5.29 (dd, 1H, $^3J_{HH}$ = 8.8, 6.1 Hz, 4-CH_{Py}), 6.06 (d, 2H, $^3J_{HH}$ = 7.6 Hz, *o*-CH_{Ar} Mg-Bn), 6.37 (d, 1H, $^3J_{HH}$ = 9.1 Hz, 5-CH_{Py}), 6.64 (t, 1H, $^3J_{HH}$ = 6.8 Hz, *p*-CH_{Ar} Mg-Bn), 7.0 (t, 2H, $^3J_{HH}$ = 6.8 Hz, *m*-CH_{Ar} Mg-Bn), 6.90–7.35 (m, 9H, *m*-C$H_{N\text{-}Ar}$, CH_{Py} Py-Bn). ^{13}C{^{1}H} NMR (C_6D_6, 25 °C, 100 MHz), δ 16.0 (*Me*-CN), 16.1 (*Me*-CN), 18.7, 18.7, 18.8, 18.9 (*o*-$Me_{N\text{-}Ar}$), 21.1, 21.2 (*p*-$Me_{N\text{-}Ar}$), 24.5 (CH_2 Mg-Bn), 38.5 (3-CH_{Py}), 44.5 (CH_2 Py-Bn), 114.0 (4-CH_{Py}), 115.4 (*p*-CH_{Ar} Mg-Bn), 121.4 (*p*-CH_{Ar} Mg-Bn), 121.4 (5-CH_{Py}), 122.8 (2-C_{Py}), 123.6 (6-C_{Py}), 123.9 (*o*-CH_{Ar} Mg-Bn), 126.6 (*p*-CH_{Ar} Py-Bn), 128.7 (*m*-CH_{Ar} Mg-Bn), 129.1 (*p*-$C_{NH\text{-}Ar}$ =C(Me)-NAr), 129.5, 129.6 (*m*-$CH_{NH\text{-}Ar}$ =C(Me)-NAr), 130.1 (*p*-$C_{N\text{-}Ar}$ C(Me)=NAr), 130.1, 130.2 (*m*-$CH_{N\text{-}Ar}$, C(Me)=NAr), 130.3 (two overlapping signals, *o*,*o*′-$C_{N\text{-}Ar}$–C(Me)=NAr), 133.3, 133.5 (*o*,*o*′-$C_{NH\text{-}Ar}$ =C(Me)-NAr), 138.7 (*i*-$C_{NH\text{-}Ar}$ =C(Me)-NAr), 140.0 (*i*-$C_{N\text{-}Ar}$ –C(Me)=NAr), 146.3 (*i*-C_{Ar} Mg-Bn), 158.6 (*i*-C_{Ar} Py-Bn), 166.1 (=C(Me)-NAr), 170.1 (–C(Me)=NAr). Complex **3b**: ^{1}H NMR (C_6D_6, 25 °C 400 MHz), δ 1.47 (s, 2H, CH_2 Mg-Bn), 1.66 (s, 6H, *Me*-CN), 1.92 (s, 12H, *o*-$Me_{N\text{-}Ar}$), 2.19 (s, 6H, *p*-$Me_{N\text{-}Ar}$), 2.91 (d, 2H, $^3J_{HH}$ = 6.5 Hz, CH_2 Py-Bn), 4.16 (tt, 1H, $^3J_{HH}$ = 6.5, 3.6 Hz, 4-CH_{Py}), 5.04 (d, 2H, $^3J_{HH}$ = 3.6 Hz, 3-CH_{Py}), 5.97 (d, 2H, $^3J_{HH}$ = 7.6 Hz, *o*-CH_{Ar} Mg-Bn), 6.62 (t, 1H, 6.9 Hz, *p*-CH_{Ar} Mg-Bn), 6.97 (t, 2H, $^3J_{HH}$ = 7.0 Hz, *m*-CH_{Ar} Mg-Bn), 7.00–7.40 (m, 11H, C$H_{N\text{-}Ar}$, CH_{Ar} Py-Bn). ^{13}C{^{1}H} NMR (C_6D_6, 25 °C, 100 MHz), δ 15.2 (*Me*-CN), 18.2 (*o*-$Me_{N\text{-}Ar}$), 18.3 (*o*-$Me_{N\text{-}Ar}$), 21.0 (*p*-$Me_{N\text{-}Ar}$), 24.2 (CH_2 Mg-Bn), 40.7 (4-CH_{Py}), 49.9 (CH_2 Py-Bn), 103.1 (3-CH_{Py}), 115.3 (*p*-CH_{Ar} Mg-Bn), 124.1 (*o*-CH_{Ar} Mg-Bn), 126.3 (*p*-CH_{Ar} Py-Bn), 127.6 (*p*-$C_{N\text{-}Ar}$), 128.6 (*m*-CH_{Ar} Mg-Bn), 129.4 (*m*-$CH_{N\text{-}Ar}$), 134.0 (*o*-$C_{N\text{-}Ar}$), 145.1 (*i*-$C_{N\text{-}Ar}$), 145.4 (2-C_{Py}), 146.4 (*i*-C_{Ar} Mg-Bn), 158.8 (*i*-C_{Ar} Py-Bn), 172.9 (Me-CN).

Preparation of 4-Bn-^{iPr}H$_2$BIP. As previously described,[12,5a] this 4-Bn-^{iPr}H$_2$BIP is formed together with the corresponding aromatized pyridine-type product 4-Bn-^{iPr}BIP in the reaction of Mn(Bn)$_2$ with ^{iPr}BIP, followed by controlled methanolysis. The following modified procedure suppresses the aromatization of such dihydropyridine, yielding the desired compound:

A THF solution of the MnBn$_2$ reagent was generated in the usual way: A J. Young Teflon-valve ampule with stirring bar was charged with 200 mg (2.2 mmol) of MnCl$_2$ and 15 mL of THF. The mixture was sonicated for 5 min, and then stirred magnetically at −60 °C. To the cool, stirred solution was added 2.3 mL of a 2.0 M solution of Mg(Cl)(Bn) in THF. The pale pink color of the mixture changed to light brown. After 10 min at −60 °C, the cooling bath was removed, and the stirring continued at room temperature for 60 min, during which time the mixture took a dark green color.

The manganous reagent solution was transferred to a suspension of ^{iPr}BIP (950 mg, 1.97 mmol) in 20 mL of toluene, stirred at −60 °C. The mixture takes a dark brown color. After 10 min, it was allowed to warm at room temperature. The stirring was continued for 70 min, after which time its color had changed to deep purple. Next, an excess of dry methanol was added, carefully avoiding any admission of air, and the resulting red solution was rigorously evaporated to dryness under vacuum for 4 h. This left a reddish oily residue that was extracted with 2 × 20 mL of hexane. The extracts were filtered through a Celite pad, and evaporated to yield 956 mg of the product 4-Bn-^{iPr}H$_2$BIP as a yellow solid. ^{1}H RMN (C_6D_6, 25 °C, 500 MHz), δ 1.07 (d, 6H, $^3J_{HH}$ = 7.1 Hz, CHMe*Me*), 1.09 (d, 6 H, $^3J_{HH}$ = 7.4 Hz, CH*Me*Me), 1.10 (d, 6H, $^3J_{HH}$ = 7.1 Hz, CHMe*Me*), 1.14 (d, 6H, $^3J_{HH}$ = 7.0 Hz, CH*Me*Me), 1.65 (s, 6H, *Me*-C=N), 2.78 (sept, 4H, $^3J_{HH}$ = 6.9 Hz, C*H*Me$_2$), 2.79 (d, $^3J_{HH}$ = 3.59 Hz, 2H, CH_2 Py-Bn), 3.75 (tt, 1H, $^3J_{HH}$ = 7.4, 3.6 Hz, 4-CH_{Py}), 5.00 (dd, 2H, $^3J_{HH}$ = 4.2 Hz, $^4J_{HH}$ = 1.6 Hz, 3- and 5-CH_{Py}), 7.11–7.14 (m, 8H, C$H_{N\text{-}Ar}$ and Py-Bn), 7.21 (m, 3H, C$H_{N\text{-}Ar}$ and Py-Bn), 8.87 (bs, 1H, NH_{Py}). ^{13}C{^{1}H} RMN (C_6D_6, 25 °C, 125 MHz), δ 15.4 (*Me*-C=N), 22.9 (CHMe*Me*), 23.3 (CH*Me*Me), 28.7 (CHMe$_2$), 28.8 (CHMe$_2$), 38.5 (4-CH_{Py}), 46.3 (CH_2 Py-Bn), 104.6 (3-CH_{Py}), 123.4 (*m*-$CH_{N\text{-}Ar}$), 124.2 (*p*-$CH_{N\text{-}Ar}$), 126.4 (*p*-CH_{Ar}, Py-Bn), 128.6 (*m*-CH_{Ar}, Py-Bn), 129.7 (*o*-CH_{Ar}, Py-Bn), 136.2 (*o*-$C_{N\text{-}Ar}$), 136.3 (*o*-$C_{N\text{-}Ar}$), 137.5 (2-C_{Py}), 139.3 (*i*-C_{Ar} Py-Bn), 146.5 (*i*-$C_{N\text{-}Ar}$), 159.7 (Me-CN).

Reaction of [Mg(Bn)$_2$THF$_2$] with 4-Bn-^{iPr}H$_2$BIP. Synthesis of 3a. A cold (−40 °C) toluene solution (5 mL) of the adduct [Mg(CH$_2$Ph)$_2$THF$_2$] (130 mg, 0.371 mmol) was added slowly to a cold (−40 °C) pentane (10 mL) yellow solution of the 4-benzyl-dihydropyridine 4-Bn-^{iPr}H$_2$BIP (206 mg, 0.360 mmol) placed in a scintillation 20 mL vial. The reaction mixture was stirred vigorously, while the color of the solution turned from yellow to clear orange. During a few minutes, the color kept gradually changing then to blue, ending up as dark red-purple. After 3 h stirring, the solution was evaporated to dryness, leaving a purple foamy residue. The ^{1}H NMR of this reaction crude showed a single set of signals corresponding to compound **3a**. The solid was redissolved in pentane (10 mL), concentrated, and stored at −20 °C. After 6 days, compound **3a** precipitated as a purple solid. Upon filtration and drying, 148.2 mg (60%) was isolated. Anal. Calcd for $C_{47}N_{57}N_3Mg$: C, 82.02; H, 8.35; N, 6.11. Found: C, 81.93; H, 8.50; N, 5.76.

Reaction of Mg(^{n}Bu)$_2$ with 4-Bn-^{iPr}H$_2$BIP. Synthesis of [Mg(^{n}Bu)(4-Bn-^{iPr}HBIP)] (4). To a cold (−60 °C) hexane yellow solution (15 mL) of the alkyl-dihydropyridine derivative 4-Bn-^{iPr}H$_2$BIP (246.9 mg, 0.430 mmol) was added a colorless solution of Mg(^{n}Bu)$_2$ (1.0 M, 0.45 mL, 0.45 mmol) in heptane. The resultant solution changed immediately to dark blue. The reaction mixture was kept cold for 10 min, the bath was then removed, and the mixture was stirred for 80 min at room temperature. The solution was taken to dryness to obtain a blue oily residue, whose ^{1}H NMR spectrum showed only signals corresponding to complex **4**. This residue was redissolved in 10 mL of pentane, concentrated to ca. 3 mL, and stored at −20 °C. The product precipitated as a microcrystalline solid that was filtered off and dried under vacuum. Yield: 191.2 mg (68%). Blue-purple crystals, suitable for X-ray diffraction studies, were obtained by careful recrystallization from pentane at −20 °C. ^{1}H NMR (C_6D_6, 25 °C 400 MHz), δ −0.50 (dd, 2H, $^3J_{HH} \approx$ 8.3 Hz, α-CH_2 Mg-^{n}Bu), 0.73 (t, 3H, δ-CH_3 Mg-^{n}Bu), 0.85 (m, 1H, β-CH*H* Mg-^{n}Bu), 0.91 (m, 1H, β-C*H*H Mg-^{n}Bu), 0.98 (d, 6H, $^3J_{HH}$ = 6.7 Hz, CHMe*Me*), 1.01 (d, 6H, $^3J_{HH}$ = 6.7 Hz, CH*Me*Me), 1.10 (m, 2H, γ-CH_2 Mg-Bu), 1.21 (d, 6H,

DOI: 10.1021/acs.organomet.6b00528
Organometallics XXXX, XXX, XXX–XXX

$^3J_{HH}$ = 6.7 Hz, CHMe*Me*), 1.22 (d, 6H, $^3J_{HH}$ = 6.7 Hz, CHMe*Me*), 1.69 (s, 6H, *Me*-CN), 2.63 (sept, 2H, $^3J_{HH}$ = 6.8 Hz, C*H*Me$_2$), 2.70 (sept, 2H, $^3J_{HH}$ = 6.8 Hz, C*H*Me$_2$), 2.93 (d, 2H, $^3J_{HH}$ = 6.8 Hz, CH_2, Py-Bn), 4.06 (m, 1H, 4-CH_{Py}), 5.14 (d, 2H, 3,3′-CH_{Py}), 6.97−7.26 (m, 11H, C$H_{N\text{-}Ar}$, CH_{Ar} Py-Bn). ^{13}C{^{1}H}-NMR (C_6D_6, 25 °C, 100 MHz), δ 7.2 (α-CH_2 Mg-^{n}Bu), 14.3 (δ-CH_3 Mg-^{n}Bu), 16.2 (*Me*-CN), 23.8 (CHMe*Me*), 23.8 (CH*Me*Me), 23.9 (CHMe*Me*), 24.0 (CH*Me*Me), 29.0 (CHMe$_2$), 29.1 (*C*HMe$_2$), 32.0 (β-CH_2 Mg-^{n}Bu), 32.2 (γ-CH_2 Mg-^{n}Bu), 40.3 (4-CH_{Py}), 47.7 (CH_2 Py-Bn), 105.3 (3-*C*H$_{Py}$), 123.9 (*m*-C$H_{N\text{-}Ar}$), 124.0 (*m*-*C*H$_{N\text{-}Ar}$), 126.1 (*o*-*C*H$_{Ar}$ Py-Bn), 126.3 (*p*-CH_{Ar} Py-Bn), 128.7 (*p*-C$H_{N\text{-}Ar}$), 130.0 (*m*-CH_{Ar} Py-Bn), 138.6 (*o*-$C_{N\text{-}Ar}$), 138.7 (*o*-$C_{N\text{-}Ar}$), 139.9 (*i*-C_{Ar} Py-Bn), 144.3 (2-C_{Py}), 145.0 (*i*-$C_{N\text{-}Ar}$), 173.7 (Me-CN). Anal. Calcd for $C_{44}H_{59}N_3Mg$: C, 80.77; H, 9.09; N, 6.42. Found: C, 80.74; H, 9.11; N, 6.14.

Monitoring the Reaction of [Mg(Bn)$_2$THF$_2$] with ^{iPr}BIP at Variable Temperature. In a nitrogen-filled glovebox, a colorless solution (0.5 mL; C_7D_8) of [Mg(Bn)$_2$THF$_2$] (6.5 mg; 0.018 mmol) was placed in a standard NMR tube. Another NMR tube was charged with 8.9 mg (0.018 mmol) of yellow ^{iPr}BIP, which was suspended in 0.5 mL of C_7D_8. Both tubes were sealed with rubber taps, taken out from the glovebox, interfaced to a vacuum/argon line, and cooled down to −65 °C. Then, under an argon atmosphere, the solution of [Mg(Bn)$_2$THF$_2$] was transferred via cannula to the fine yellow suspension of ^{iPr}BIP at the above-mentioned temperature. The NMR tube was gently shaken, and the color of the mixture turned rapidly to green. The tube was transferred to the NMR probe, which had been precooled at −65 °C. ^{1}H NMR spectra were recorded at different temperatures from −60 to 25 °C. The first ^{1}H NMR spectrum (at the lowest temperature) showed a new set of signals different from those of the starting materials, evidencing that a first transformation had reached completion. The main signals of the spectrum were attributed to the complex [Mg(Bn)(2-Bn-^{iPr}HBIP), ***Int* a**. ^{1}H NMR (toluene-d_8. −50 °C, 400 MHz), δ 1.00 (bs, 3H, CH*Me*), 1.08 (bs, 3H, CH*Me*), 1.13 (bs, 3H, CH*Me*), 1.21 (bs, 3H, CH*Me*), 1.22 (bs, 3H, CH*Me*), 1.23 (bs, 3H, CH*Me*), 1.27 (bs, 3H, CH*Me*), 1.71 (bs, 3H, CH*Me*), 1.73 (bs, 3H, *Me*-CN), 1.78 (bs, 3H, *Me*-CN), 2.24 (bd, 1H, $^2J_{HH}$ = 14.0 Hz, CH*H* C2$_{Py}$-Bn), 2.60 (bs, 1H, C*H*Me$_2$), 2.82 (bs, 1H, C*H*Me$_2$), 3.41 (bs, 1H, C*H*Me$_2$), 3.62 (bs, 1H, C*H*Me$_2$), 4.27 (bd, 1H, $^2J_{HH}$ = 14.0 Hz, C*H*H C2$_{Py}$-Bn), 4.89 (bs, 1H, 3CH_{Py}), 5.77 (bs, 1H, 5CH_{Py}), 5.89 (bs, 2H, *o*-CH_{Ar} Mg-Bn), 6.47 (bs, 1H, CH_{Ar} 4CH_{Py}), 6.61 (bs, 1H, *p*-CH_{Ar} Mg-Bn) 6.90 (hidden, 2H, *m*-CH_{Ar} Mg-Bn) 6.90−7.40 (m, 11H, CH_{Ar}).

X-ray Structure Analyses for 1b, [Mg(Bn)$_2$THF$_2$], and 4. Crystals were coated with dry perfluoropolyether, mounted on glass fibers, and fixed in a cold nitrogen stream (T = 100 K) to the goniometer head. Data collection was performed on a Bruker-Nonius X8Apex-II CCD diffractometer, using monochromatic radiation λ(MoKα) = 0.71073 Å, by means of ω and φ scans with a width of 0.50°. The data were reduced (SAINT)[22,23] and corrected for absorption effects by the multiscan method (SADABS).[24] The structure was solved by direct methods (SIR-2002)[25] and refined against all F^2 data by full-matrix least-squares techniques (SHELXTL-6.12)[25] minimizing $w[F_o^2 - F_c^2]^2$. Crystal data for **1b**, [**Mg(Bn)$_2$(THF)$_2$**], and **4** are given in the Supporting Information (see Table S1).

■ ASSOCIATED CONTENT

Supporting Information

The Supporting Information is available free of charge on the ACS Publications website at DOI: 10.1021/acs.organomet.6b00528.

Figures S1 and S2 show the ^{1}H NMR spectra of compounds **1a** and the mixture of compounds **2a** and **3a**, respectively. Figures S3−S6 show ORTEP drawings, and a summary of crystallographic data is included in Table S1 (PDF)

Crystallographic data for **1b**, [Mg(Bn)$_2$(THF)$_2$], and **4** (CIF)

■ AUTHOR INFORMATION

Corresponding Authors

*E-mail: antonior@iiq.csic.es (A.R.-D.).

*E-mail: campora@iiq.csic.es (J.C.).

Notes

The authors declare no competing financial interest.

■ ACKNOWLEDGMENTS

The Spanish Ministry of Economy and Innovation (MINECO) and the FEDER funds of the European Union (CTQ2015-68978-P) supported this work. J.J.S gratefully thanks MICINN for a PFPI postgraduate studentship.

■ REFERENCES

(1) For leading reviews: (a) Gibson, V. C.; Redshaw, C.; Solan, G. A. *Chem. Rev.* **2007**, *107*, 1745−1776. (b) Knijnenburg, Q.; Gambarotta, S.; Budzelaar, P. H. M. *Dalton Trans.* **2006**, 5442−5448. (c) Flisak, Z.; Sun, W.-H. *ACS Catal.* **2015**, *5*, 4713−4724.

(2) Recent examples: (a) Cartes, M. A.; Rodríguez-Delgado, A.; Palma, P.; Álvarez, E.; Cámpora, J. *Organometallics* **2014**, *33*, 1834−1839. (b) Antonov, A. A.; Samsonenko, D. G.; Talsi, E. P.; Bryliakov, K. P. *Organometallics* **2013**, *32*, 2187−2191. (c) Hojilla Atienza, C. C.; Milsmann, C.; Semproni, S. P.; Turner, Z. R.; Chirik, P. J. *Inorg. Chem.* **2013**, *52*, 5403−5417. (d) Obligacion, J. V.; Chirik, P. J. *J. Am. Chem. Soc.* **2013**, *135*, 19107−19110. (e) Hojilla Atienza, C. C.; Milsmann, C.; Lobkovsky, E.; Chirik, P. J. *Angew. Chem., Int. Ed.* **2011**, *50*, 8143−8147. (f) Pérez, C. M.; Rodríguez-Delgado, A.; Palma, P.; Álvarez, E.; Gutiérrez-Puebla, E.; Cámpora, J. *Chem.—Eur. J.* **2010**, *16*, 13834−13842.

(3) (a) Cartes, M. Á.; Rodríguez-Delgado, A.; Palma, P.; Sánchez, L. J.; Cámpora, J. *Catal. Sci. Technol.* **2014**, *4*, 2504−2507. (b) Bryliakov, K. P.; Talsi, E. P.; Semikolenova, N. V.; Zakharov, V. A. *Organometallics* **2009**, *28*, 3225−3232. (c) Bouwkamp, M. W.; Lobkovsky, E.; Chirik, P. J. *J. Am. Chem. Soc.* **2005**, *127*, 9660−9661. (d) Humphries, M. J.; Tellmann, K. P.; Gibson, V. C.; White, A. J. P.; Williams, D. J. *Organometallics* **2005**, *24*, 2039−2050. (e) Kleigrewe, N.; Steffen, W.; Blömker, T.; Kehr, G.; Fröhlich, R.; Wibbeling, B.; Erker, G.; Wasilke, J.-C.; Wu, G.; Bazan, G. *J. Am. Chem. Soc.* **2005**, *127*, 13955−13968.

(4) See, for example: (a) Chirik, P. J. *Acc. Chem. Res.* **2015**, *48*, 1687−1695. (b) Biernesser, A. B.; Li, B.; Byers, J. A. *J. Am. Chem. Soc.* **2013**, *135*, 16553−16560. (c) Karpiniec, S. S.; McGuinness, D. S.; Britovsek, G. P.; Patel, J. *Organometallics* **2012**, *31*, 3439−3442. (d) Tondreau, A. M.; Lobkovsky, E.; Chirik, P. J. *Org. Lett.* **2008**, *10*, 2789−2792. (e) Atienza, C. C. H.; Diao, T.; Weller, K. J.; Nye, S. A.; Lewis, K. M.; Delis, J. G. P.; Boyer, J. L.; Roy, A. K.; Chirik, P. J. *J. Am. Chem. Soc.* **2014**, *136*, 12108−12118.

(5) (a) Sandoval, J. J.; Palma, P.; Álvarez, E.; Rodríguez-Delgado, A.; Cámpora, J. *Chem. Commun.* **2013**, *49*, 6791−6794. (b) Arrowsmith, M.; Hill, M. S.; Kociok-Köhn, G. *Organometallics* **2010**, *29*, 4203−4206. (c) Blackmore, I. J.; Gibson, V. C.; Hitchcock, P. B.; Rees, C. W.; Williams, D. J.; White, A. J. P. *J. Am. Chem. Soc.* **2005**, *127*, 6012−6020.

(6) (a) Tay, B.-Y.; Wang, C.; Chia, S.-C.; Stubbs, L. P.; Wong, P.-K.; van Meurs, M. *Organometallics* **2011**, *30*, 6028−6033. (b) Knijnenburg, Q.; Smits, J. M. M.; Budzelaar, P. H. M. *Organometallics* **2006**, *25*, 1036−1046. (c) Scott, J.; Gambarotta, S.; Korobkov, I.; Knijnenburg, Q.; de Bruin, B.; Budzelaar, P. H. M. *J. Am. Chem. Soc.* **2005**, *127*, 17204−17206. (d) Knijnenburg, Q.; Smits, J. M. M.; Budzelaar, P. H.M. *C. R. Chim.* **2004**, *7*, 865−867. (e) Bruce, M.; Gibson, V. C.; Redshaw, C.; Solan, G. A.; White, A. J. P.; Williams, D. J. *Chem. Commun.* **1998**, 2523−2525.

(7) (a) Budzelaar, P. H. M. *Eur. J. Inorg. Chem.* **2012**, *2012*, 530−534. (b) Sieh, D.; Schlimm, M.; Andernach, L.; Angersbach, F.; Nückel, S.; Schöffel, J.; Šušnjar, N.; Burger, P. *Eur. J. Inorg. Chem.* **2012**, *2012*, 444−462.

DOI: 10.1021/acs.organomet.6b00528
Organometallics XXXX, XXX, XXX−XXX

(8) (a) Bouwkamp, M. W.; Bart, S. C.; Hawrelak, E. J.; Trovitch, R. J.; Lobkovsky, E.; Chirik, P. J. *Chem. Commun.* **2005**, 3406−3408. (b) Cámpora, J.; Naz, A. M.; Palma, P.; Álvarez, E.; Reyes, M. L. *Organometallics* **2005**, *24*, 4878−4881.
(9) (a) Scott, J.; Gambarotta, S.; Korobkov, I.; Budzelaar, P. H. M. *Organometallics* **2005**, *24*, 6298−6300. (b) Fernández, I.; Trovitch, R. J.; Lobkovsky, E.; Chirik, P. J. *Organometallics* **2008**, *27*, 109−118.
(10) (a) Kooistra, T. M.; Knijnenburg, Q.; Smits, J. M. M.; Horton, A. D.; Budzelaar, P. H. M.; Gal, A. W. *Angew. Chem., Int. Ed.* **2001**, *40*, 4719−4722. (b) Gibson, V. C.; Humphries, M. J.; Tellmann, K. P.; Wass, D. F.; White, A. J. P.; Williams, D. J. *Chem. Commun.* **2001**, 2252−2253. (c) Zhu, D.; Janssen, F. F. B. J.; Budzelaar, P. H. M. *Organometallics* **2010**, *29*, 1897−1908. (d) Zhu, D.; Thapa, I.; Korobkov, I.; Gambarotta, S.; Budzelaar, P. H. M. *Inorg. Chem.* **2011**, *50*, 9879−9887.
(11) (a) Sugiyama, H.; Aharonian, G.; Gambarotta, S.; Yap, G. P. A.; Budzelaar, P. H. M. *J. Am. Chem. Soc.* **2002**, *124*, 12268−12269. (b) Reardon, D.; Aharonian, G.; Gambarotta, S.; Yap, G. P. A. *Organometallics* **2002**, *21*, 786−788.
(12) Cámpora, J.; Pérez, C. M.; Rodríguez-Delgado, A.; Naz, A. M.; Palma, P.; Álvarez, E. *Organometallics* **2007**, *26*, 1104−1107.
(13) (a) Pyykkö, P.; Atsumi, M. *Chem.—Eur. J.* **2009**, *15*, 12770−12779. (b) Pyykkö, P. *J. Phys. Chem. A* **2015**, *119*, 2326−2337.
(14) Hill, M. S.; Liptrot, D. J.; Weetman, C. *Chem. Soc. Rev.* **2016**, *45*, 972−988.
(15) Schrock, R. R. *J. Organomet. Chem.* **1976**, *122*, 209−225.
(16) Defined as $\tau_4 = [360 - (a + b)]/(360 - 2q)$, where a and b are the two largest valence angles at the coordination center, and q is the ideal tetrahedral angle, 109.5°. Yang, L.; Powell, D. R.; Houser, R. P. *Dalton Trans.* **2007**, 955−964.
(17) Thompson, E. J.; Myers, T. W.; Berben, L. A. *Angew. Chem., Int. Ed.* **2014**, *53*, 14132−14134.
(18) (a) Mani, N. S.; Beall, L. S.; Miller, T.; Anderson, O. P.; Hope, H.; Parkin, S. R.; Williams, D. J.; Barrett, A. G.; Hoffman, B. M. *J. Chem. Soc., Chem. Commun.* **1994**, 2095−2096. (b) Chandra, T.; Kraft, B. J.; Huffman, J. C.; Zaleski, J. M. *Inorg. Chem.* **2003**, *42*, 5158−5172.
(19) (a) Nimitsiriwat, N.; Gibson, V. C.; Marshall, E. K.; Takolpuckdee, P.; Tomov, A. L.; White, A. J. P.; Williams, D. J.; Elsegood, M. R. J.; Dale, S. H. *Inorg. Chem.* **2007**, *46*, 9988−9997.
(20) The Mg−C distance in **4** is longer than in any other benzylmagnesium complex recorded in the Cambridge Structural Database (vers. 5.37, Nov. 2015).
(21) Scott, J.; Gambarotta, S.; Korobkov, I.; Budzelaar, P. H. M. *J. Am. Chem. Soc.* **2005**, *127*, 13019−13029.
(22) *APEX2*; Bruker AXS, Inc.: Madison, WI, 2007.
(23) *APEX2*; Bruker AXS, Inc.: Madison, WI, 2001.
(24) Burla, C. M.; Camalli, M.; Carrozzini, B.; Cascarano, G. L.; Giacovazzo, G.; Polidori, R.; Spagna, R. SIR2002: the program. *J. Appl. Crystallogr.* **2003**, *36*, 1103−1103.
(25) Sheldrick, G. M. *Acta Crystallogr., Sect. A: Found. Crystallogr.* **2008**, *A64*, 112−122.

DOI: 10.1021/acs.organomet.6b00528
Organometallics XXXX, XXX, XXX−XXX